

Survey for Transiting Extrasolar Planets in Stellar Systems. II. Spectrophotometry and Metallicities of Open Clusters

J. L. Marshall, Christopher J. Burke, D. L. DePoy, Andrew Gould, & Juna A. Kollmeier

Department of Astronomy, The Ohio State University

140 West 18th Avenue, Columbus, Ohio 43210-1173

marshall@astronomy.ohio-state.edu, cjburke@astronomy.ohio-state.edu,

depoy@astronomy.ohio-state.edu, gould@astronomy.ohio-state.edu,

jak@astronomy.ohio-state.edu

ABSTRACT

We present metallicity estimates for seven open clusters based on spectrophotometric indices from moderate-resolution spectroscopy. Observations of field giants of known metallicity provide a correlation between the spectroscopic indices and the metallicity of open cluster giants. We use χ^2 analysis to fit the relation of spectrophotometric indices to metallicity in field giants. The resulting function allows an estimate of the target-cluster giants' metallicities with an error in the method of ± 0.08 dex. We derive the following metallicities for the seven open clusters: NGC 1245, $[m/H] = -0.14 \pm 0.04$; NGC 2099, $[m/H] = +0.05 \pm 0.05$; NGC 2324, $[m/H] = -0.06 \pm 0.04$; NGC 2539, $[m/H] = -0.04 \pm 0.03$; NGC 2682 (M67), $[m/H] = -0.05 \pm 0.02$; NGC 6705, $[m/H] = +0.14 \pm 0.08$; NGC 6819, $[m/H] = -0.07 \pm 0.12$. These metallicity estimates will be useful in planning future extra-solar planet transit searches since planets may form more readily in metal-rich environments.

Subject headings: Galaxy: Open Clusters and Associations: General, Galaxy: Abundances, Galaxy: Kinematics and Dynamics, Stars: Abundances

1. Introduction

Galactic open clusters occupy a wide range of ages, sizes, locations in the Galaxy, initial mass functions, and metallicities, and are found throughout the Galactic disk. Thus, open clusters are excellent tracers of Galactic disk properties and give insight into the formation of the disk (Janes & Adler 1982; Janes & Phelps 1994; Friel 1995; de La Fuente Marcos & de La Fuente Marcos 2004). Unfortunately, the fundamental properties of open clusters

are difficult to determine. Current estimates of these properties vary widely; there is only marginal agreement in the literature about the age, metallicity, reddening, or Galactocentric distance of any given open cluster. Part of the disparity between estimates is due to the variety of methods used to determine these quantities. The published metallicity estimates of an open cluster are especially prone to disagreement because each technique has different sensitivities to metallicity patterns, and it is likely that none of the methods, with the possible exception of high-resolution spectroscopy, commonly used to estimate stellar metallicity is measuring the “true” metallicity of the stars. Additionally, the relationship between the many different techniques is often unknown. The past few decades have yielded significant advances in the study of open clusters, but there is still much work to be done toward determining the fundamental properties of the more than 1500 currently known Galactic open clusters.

Nonetheless, open clusters are extremely useful objects to study because each cluster represents a homogeneous set of stars. All stars in an open cluster form at the same time and in the same circumstances, and thus are expected to have the same age, metallicity, and Galactocentric distance. For this reason, open clusters are good testbeds for many types of Galactic studies. For example, they may be ideal objects in which to search for extra-solar planets (e.g., Gonzalez 1997). Furthermore, open clusters can be metal-rich objects. Metal-rich environments have recently received attention due to the suggestion (e.g., Santos et al. 2000; Gonzalez & Laws 2000) that extra-solar planets form more readily around metal-rich stars. If this is the case, metal-rich open clusters may be excellent places to search for extra-solar planets. This is the primary motivation for this work; planet searches will be conducted in metal-rich open clusters identified in this study. These programs will be carried out by the Survey for Transiting Extrasolar Planets in Stellar Systems (STEPSS) program (e.g. Burke et al. 2003).

In this paper we present new, accurate metallicity estimates for seven open clusters that were presumed to be metal-rich based on literature searches. We have obtained moderate resolution spectroscopy of giants in the target-clusters and use spectrophotometric line indices to produce metallicity estimates for the target-clusters.

2. Observational Procedure

In this work we follow the method of Friel (1987) to determine metallicities using spectrophotometric line indices as proxies for high-resolution metallicity estimates. This procedure was adopted in several subsequent papers, including Thogerson et al. (1993), Friel & Janes (1993), and most recently Friel et al. (2002). Here we quantitatively assess the

precision of this methodology, which is described below.

2.1. Sample Selection

The target-clusters were selected as a precursor to a search for extra-solar planets. Clusters to be observed were chosen on the basis of a high metallicity estimate cited in the literature, as well as their location in the Galaxy. We used the Lynga (1987) database to select target-clusters, with selection criteria of $[\text{Fe}/\text{H}] > -0.2$ so as not to exclude metal-rich clusters with large errors in their metallicity determination. We required the target-clusters to have distances > 300 pc, so that the stars would be bright enough to observe on our 2-m class telescopes, and to have declinations δ (1950) $> -15^\circ$, so as to be observable from the northern hemisphere. We did not put any constraints on the ages of the clusters; indeed, the selected open clusters span a wide range of ages. These criteria yielded a set of 26 candidate open clusters.

These target-clusters were observed with the MDM “Echelle” CCD imager at the 1.3 m McGraw-Hill telescope of the MDM Observatory¹ in a preliminary observing run. During this run we obtained images of the target-clusters as well as instrumental color-magnitude diagrams (CMDs) of each cluster. We use these images and instrumental CMDs to select target-cluster stars.

Using these preparatory images, we further required the selected open clusters to be optically distinguishable as a cluster in the 1.3 m images (the imager has a 17' field of view). This constraint ensures a large number of observable stars, both in the clump (for this work) and in the cluster in general (for use in the planet searches). The clusters were also explicitly required to have several giant stars in or near the clump, based on the instrumental CMD, in order to determine accurately the metallicity of each target-cluster. The seven target-clusters selected from these criteria are NGC 1245, NGC 2099, NGC 2324, NGC 2539, NGC 2682, NGC 6705, and NGC 6819. We select giants with $(B - V)_0 \approx 1$ (typically red clump giants) in each of the target-clusters. For reference, the names of the stars in each target-cluster used here are those given in the WEBDA open cluster database². We also give the references for the identifications for each cluster in §4.2

We also observed stars of known metallicity to use as calibrators. We took calibration stars mainly from the survey of Friel (1987), who presents a large sample of bright field stars

¹See <http://www.astro.lsa.umich.edu/obs/mdm/>

²See <http://obswww.unige.ch/webda/>

and cluster giants with accompanying measured indices and previously derived metallicities. We took bright metal-poor calibration stars from Cottrell & Sneden (1986), while additional giant stars from the old open cluster NGC 2682 were taken from Friel & Janes (1993). In order to minimize calibration errors between target-cluster stars and the calibrators, we selected calibration stars from these papers that have a color of $B - V = 1 \pm 0.1$ mag, roughly the same (dereddened) color as the target-cluster stars. Additionally, we observed a few calibration stars with $B - V < 0.9$, in order to ensure some overlap with the color of the target-cluster stars.

2.2. Observations and Data Reduction

The spectral data were obtained at the MDM Observatory using the CCDS spectrograph³. We obtained one night of data (2002 January 31) on the 2.4 m Hiltner telescope, while the other seven nights of data (during 2002 March 21 - April 01) were obtained on the 1.3 m McGraw-Hill telescope. The spectra cover the wavelength range 3800-5400 Å with the 350 l/mm (1.33 Å/pix) grating. The full-width at half-maximum (FWHM) of an unresolved emission line is ~ 3 pixels, yielding a spectral resolution ($\lambda/\Delta\lambda$) of ~ 1150 . All spectra on both telescopes use an 87 μm slit for uniformity. This slit size translates to $1''$ on the 2.4 m and $1''.8$ on the 1.3 m. Most spectra have formal signal-to-noise ratios (S/N) $\gtrsim 100$ per pixel.

We observed the target-cluster stars interspersed with calibration stars of known metallicity. Thirty-five observations of 33 target-cluster stars and 56 observations of 38 calibration stars were made. Figures 1 – 7 show the reduced spectra of all of the stars observed in each target-cluster. Figure 8 shows a selected sample of the calibration stars observed. Multiple observations of some stars were included in order to ensure reproduction of Friel’s method, to check repeatability of the measurements between telescopes, and also to have many measurements on which to base the calibration.

We reduced the data using standard IRAF⁴ routines following the usual practice of overscan subtraction, division by a flat field, and extraction of the spectra. Flat fields and comparison lamp spectra were obtained using lamps within the instrument. We correct the spectra for atmospheric extinction using the standard KPNO (Kitt Peak) extinction curves provided by IRAF.

³See <http://www.astronomy.ohio-state.edu/MDM/CCDS/>

⁴IRAF is distributed by the National Optical Astronomy Observatory, which is operated by the Association of Universities for Research in Astronomy, Inc., under cooperative agreement with the National Science Foundation.

On each night we observed a spectrophotometric standard star from Strom (1977). The application of only one standard per night (regardless of the airmass of the observations) may introduce a small color effect into the spectra since the airmass has a color term and we do nothing to account for the airmass of the observations. Due to the nature of the measurements (indices with continuum bands on either side of the lines), this is not a significant concern. No attempt was made to do spectrophotometry, i.e., we did not align the slit with the parallactic angle at each telescope pointing. This seems to have had little effect on our results.

2.3. Measurement of Spectrophotometric Indices

Several recent papers (e.g. Strader & Brodie 2004) use spectrophotometric indices as an estimator for the metallicity and other properties of individual stars. The indices are measured for both the program stars as well as calibration stars with well-known metallicity; the calibration star data are fit to obtain a calibration for the metallicities of the target-cluster stars. This practice is desirable because the indices may be measured with moderate resolution spectra to obtain a relatively accurate (i.e., generally good to ~ 0.15 dex) metallicity estimate for the star, and obviates the need for difficult-to-obtain high-resolution spectroscopy. Lick indices (Burstein et al. 1984) are commonly used in this technique and are applied to extragalactic sources for which it is often impossible to obtain high S/N, high-resolution spectra. Friel (1987) slightly altered the Lick indices to account for differences between Galactic and extragalactic sources and applied them to giant stars in the Galaxy.

The indices are defined as a ratio between a bandpass that incorporates several strong metal lines and continuum measurements on either side of this bandpass that include little flux from metal lines. The final measured indices (several per star) may then be combined to yield a metallicity estimate for each star. For example, the Fe4680 index is defined as

$$\text{Fe4680} = -2.5 \log \frac{\int_{4636.00}^{4723.00} F_{\lambda} d\lambda / 87 \text{\AA}}{\int_{4606.00}^{4636.00} F_{\lambda} d\lambda / 30 \text{\AA} + \int_{4736.00}^{4773.00} F_{\lambda} d\lambda / 37 \text{\AA}}. \quad (1)$$

The line and continuum regions of the indices used in this work are given in Table 1, as well as the species measured by each index. This table is reproduced from Friel (1987).

Figure 9 shows a sample moderate resolution spectrum obtained on the MDM 2.4 m telescope. The central bandpasses of each measured index are shown across the bottom of the figure. Figure 10 shows an enlarged section of the same spectrum, showing the central bandpass and accompanying continuum bandpasses for the Fe4680 index.

3. Analysis

3.1. Metallicities of Calibration Stars

Although the calibration stars are selected from Friel (1987), Cottrell & Sneden (1986), and Friel & Janes (1993), many of these stars have more recent metallicity estimates than those cited in these original references. In order to minimize errors introduced into our analysis from the calibration stars, we selected only field giants from Friel (1987) that had metallicity estimates from a single source. Specifically, we chose metallicity estimates from the Cayrel de Strobel et al. (2001) (hereafter CdS) catalog. This catalog is a compilation of previously published atmospheric parameters determined from high-resolution, high S/N spectra from a variety of sources. The 2001 version of the catalog contains bright F, G, and K stars in the Galactic field as well as in certain associations. We selected thirty-eight metallicity standards from Friel (1987) that had at least one metallicity determination in the CdS catalog; we obtained 56 measurements of these 38 stars.

For stars with more than one entry in the CdS catalog we combine the available entries as follows. If there are two entries we average the two quoted metallicities. For stars with three or more entries, we discard metallicity measurements more than one standard deviation away from the median of all the measurements. We then average the remaining measurements. When only one measurement was present in the catalog, we adopt it.

Many of the entries in CdS do not have associated error estimates; those that do are of order 0.1 dex. We estimate errors by finding the standard deviation of the remaining metallicities once spurious measurements are discarded as described above. For stars with only one or two measurements, or those for which only two measurements remained, we assume an error of 0.1 dex. However, this may be an overestimate of these errors, as our method reproduces metallicities of most of these field stars to higher precision (see §4.1).

3.2. The Indices: Reproducibility and Comparison to Previous Index Measurements

Table 2 gives the measured indices of the calibration stars observed in this work along with their V mag and $B-V$ colors (from the Hipparcos Catalog, ESA 1997) and metallicities (derived from the CdS database, as described above). Table 3 shows these data for the target-cluster stars.

We obtained all of the spectra with the CCDS spectrometer, and we made most of the observations with the MDM 1.3 m telescope. Since all measurements were obtained

with the same instrument, we do not expect large systematic differences between the data obtained on each telescope. Several stars were observed on both of the MDM Observatory telescopes. We compared the indices for the stars observed on both telescopes; the results are shown in Table 4. The average difference between the target-cluster stars measured on the two telescopes is 0.00 and the standard deviation between the stars measured on each telescope is 0.03. This difference is well within the errors of the measurements and suggests no systematic difference in the indices measured on the two telescopes.

We also observed some stars twice on the 1.3 m run. We compare the indices for the stars observed twice on the 1.3 m run, as well as the indices of the stars observed multiple times over both runs. No stars were observed twice on the 2.4 m run. The results are again shown in Table 4. Note that in both cases the average difference between any two measurements is 0.00. The standard deviation for the stars measured twice during the 1.3 m run is 0.04 while that for all stars measured twice (over both runs) is 0.03.

Finally, we compare our measured indices for the calibration stars to those given in Friel (1987). For all of the stars that were measured both by Friel (1987) and in this work, we found the difference between Friel’s value of each index and ours and computed the average and standard deviation for all of the indices. Our indices reproduce Friel’s well; the average difference of the indices is -0.012 and the standard deviation is 0.054.

3.3. Reddening

In order to determine quantitatively if the interstellar reddening to the target-clusters affects our results, we simulated the effects of reddening on a sample spectrum. We used IRAF utilities to redden artificially the spectra and measured the effect of reddening on each of the indices. We applied an $E(B-V)$ of 1.0 (much more extreme than any of the target-clusters should actually have; see footnotes to Table 3), and re-calculated the index values. For some indices the difference in the index between the raw spectrum and the dereddened spectrum was higher than the others (Ca4226 and G-band were 0.05 and 0.11 respectively). For the remaining nine indices the difference was 0.03 or less (roughly the precision of the index measurements). However, none of the target-clusters have nearly this high of a reddening value (see the footnotes to Table 3). At the approximate reddening values applicable to our target-clusters, the effect of reddening was well below the other sources of error. We conclude that reddening does not significantly affect our results.

4. Results

4.1. Fit to Calibrators

We begin by writing the predicted metallicity as a linear function of the 11 observed spectrophotometric line indices f_i ($i = 1 \dots 11$), $[\text{Fe}/\text{H}]_{\text{pred}} = \sum_{i=0}^{11} a_i f_i$, where $f_0 = 1$. We determine the coefficients a_i by making a linear fit to 56 stars that have spectroscopically determined metallicities from CdS of $[\text{Fe}/\text{H}] > -1.5$.

We determine which of these 11 spectrophotometric line indices are redundant as follows. In the fit we arbitrarily assign each index an error of unity. Since there are $56 - 12 = 44$ degrees of freedom (dof), the resulting χ^2/dof of the fit gives the (square of the) scatter about the fit. We then try removing each of the 12 parameters in succession and find the parameter that causes χ^2 to increase by the least. Since the number of dof has also increased (by 1), the χ^2/dof may have increased or decreased. If it has decreased, we regard the parameter as redundant, remove it, and then try removing each of the remaining 11 parameters. We continue this process until χ^2/dof begins to increase.

We derive the metallicities of the target-clusters using the 56 calibrator stars. We find that the target-cluster stars all have $[\text{Fe}/\text{H}] > -0.7$. Further, we find that thirteen calibrator stars have extremely high scatter in this fit ($\sigma > 0.15$), possibly due to large errors in their CdS metallicity determinations. We therefore repeat the entire procedure but restricted to the sample of 43 calibrator star measurements that have $[\text{Fe}/\text{H}] > -0.7$, discarding the high-scatter stars. In this case, we find 5 indices are removed (Fe4530, Fe5011, Mg, Fe5270, Fe5335). The equation used to combine the indices and produce the metallicities of the stars is

$$\begin{aligned}
 [m/H] = & \\
 & -3.180415 + 4.398434 \times \text{Fe4065} + 1.105911 \times \text{CN4216} + \\
 & -2.480848 \times \text{Ca4226} + -0.725162 \times \text{G-band} + \\
 & 2.835423 \times \text{Fe4680} + -1.620898 \times \text{Fe4920}.
 \end{aligned}
 \tag{2}$$

The coefficients of the indices are also presented in Table 5.

The scatter about the relation is $\sqrt{\chi^2/\text{dof}} = 0.0709$. This number reflects the quadrature sum of the root-mean-square (rms) error in the spectroscopic metallicities and the intrinsic scatter of the method.

Even though the target-cluster giants are selected to have approximately the same $B-V$ color as the calibration stars, we find that the derived metallicities of the target-cluster giants

have a non-negligible dependence on color. This effect is due to the fact that some of the stars we observed were not in the red giant clump but rather were more evolved stars on the giant branch. Thus these stars have different surface temperatures and gravities than the rest of our clump stars. This effect is readily calibrated by removing the color dependence of the metallicity.

We compare metallicity residual (relative to CdS metallicity) to $B - V$ color for the five calibrator stars and five target-cluster stars in NGC 2682 (the target-cluster with the most well-determined metallicity in the literature). The $B - V$ colors of these stars are dereddened using $E(B-V)=0.05$ (Montgomery et al. 1993). For the five program giants (with no literature metallicity values) we assume the average literature value for the cluster metallicity of $[Fe/H]=-0.05$. The equation of the fit is

$$[Fe/H]_{CdS} - [m/H]_{thispaper} = 1.4937 \times (B - V) - 1.5858. \quad (3)$$

The derived color correction is then applied to the 35 target-cluster stars individually to obtain the final metallicity of each star. We assume that the spread in ages of the target-clusters has a negligible effect on this fit. More explicitly, we assume the errors associated with this assumption are smaller than our other sources of error. The data and the derived fit are shown in Figure 11.

Figure 12 compares our derived metallicities (after applying the color correction) to those of CdS. The scatter in this relation is ~ 0.08 dex, which is only 0.01 dex larger than the scatter in the derivation of the original relation. We therefore estimate the overall error in the method to be ~ 0.08 dex. This implies that the technique of applying a color correction to the derived metallicities produces acceptable results.

Note that we use the term $[m/H]$ to refer to our metallicity estimates. Since each of the spectrophotometric line indices is selected to incorporate several metal absorption lines, our method must measure some aspect of the star’s metallicity. But since the indices comprise several different metal species, this method does not necessarily measure only the iron abundance of the star.

4.2. Cluster Metallicities and Comparison to Previous Determinations

Table 6 shows the metallicities determined for each of the target-cluster stars, the mean metallicities of each target-cluster, and the scatter in the target-cluster star metallicities. We report the error for each target-cluster as the error in the mean of the target-cluster giant

stars: the error in the method (0.08 dex) divided by the square root of the number of giant stars measured in each target-cluster.

Note that our method differs in a significant way from previous papers using spectrophotometric line indices to derive metallicities: we combine all of the measured indices at once using χ^2 analysis, whereas others (e.g., Friel & Janes 1993; Thogerson et al. 1993; Friel et al. 2002) use each index individually to derive a metallicity for each star, then average the derived metallicities together. Our analysis indicates that several of the indices provide no additional sensitivity to metallicity for the stars in our sample, and we do not use them at all.

Below we discuss the application of our fit to each target-cluster individually and compare the derived metallicity to existing values in the literature. Most of the open clusters studied here do not have a large number of previous metallicity determinations.

A new catalog of open clusters (Dias et al. 2002) improves upon and replaces the Lynga (1987) database and includes metallicity estimates for all of our target-clusters. Although the on-line catalog does not include references for the metallicity estimates of the clusters, Dias (2005, private communication) has provided the references used in the catalog. We cite the references given to us by Dias for each of the clusters in the discussion below.

4.2.1. NGC 1245

NGC 1245 has a metallicity of $[m/H] = -0.14 \pm 0.04$ derived from seven measurements of six stars. The scatter in the derived metallicities is 0.09 dex, close to what we expect based on the error in the method. The identifiers used in Table 3 are taken from Chincarini (1964). The cluster has a well-defined red clump and all target-cluster stars were taken from the clump. We observed seven of the 27 clump giants from our instrumental CMD of NGC 1245. Unfortunately, WEBDA does not give membership probabilities for these stars.

NGC 1245 is studied extensively by Burke et al. (2004) (hereafter referred to as Paper I); new photometry is reported and fundamental properties of the cluster are derived, including a new metallicity value based on color-magnitude diagram profile fitting. It was selected as the first of several clusters for a targeted transiting planet search by the STEPSS program. Paper I reports a metallicity for NGC 1245 of $[Fe/H] = -0.05 \pm 0.03$ (statistical) ± 0.08 (systematic). This value is derived from detailed isochrone fitting, using a χ^2 fit to accurate photometric observations to derive physical parameters of the cluster and quantifying the systematic errors in the method. This method yields perhaps the most reliable derivation of cluster parameters of any of those referred to below, with the possible exception of the

high-resolution spectroscopy determinations.

It should be noted that in §3.1 of Paper I a best-fit value of the total-to-selective extinction $R_V=2.3$ is derived, yielding a metallicity of $[\text{Fe}/\text{H}]=-0.26$. This value was in fact not used in the determination as it was assumed to be too low and the fiducial value of $R_V=3.2$ is adopted. Our derived metallicity agrees equally well with both determinations of Paper I. The assumed total-to-selective extinction may often be a large source of error in the determination of fundamental cluster parameters using isochrone fitting methods, since R_V is not 3.2 uniformly throughout the Galaxy (see, e.g., Gould et al. 2001).

Wee & Lee (1996) also study the metallicity of NGC 1245 with Washington photometry. They derive a metallicity of $[\text{Fe}/\text{H}]=-0.04\pm 0.05$. Gratton (2000) cite a value of $[\text{Fe}/\text{H}]=+0.1\pm 0.15$, derived by applying corrections based on high-resolution spectroscopy to low-resolution metallicity determinations.

The metallicity of NGC 1245 derived here, $[\text{m}/\text{H}]=-0.14\pm 0.04$, is somewhat lower than previously published metallicities for this cluster. In particular, our metallicity for NGC 1245 reproduces the value cited in Paper I to only ~ 2 sigma. We agree with the Gratton (2000) metallicity to 1.5 sigma and the Wee & Lee (1996) metallicity to 1.6 sigma.

4.2.2. NGC 2099

The metallicity of NGC 2099 is $[\text{m}/\text{H}]=+0.05\pm 0.05$ and is derived from measurements of eight stars. The metallicity determinations of the target-cluster stars in NGC 2099 have a scatter of 0.14 dex, about twice what we expect. Target-cluster names in Table 3 are taken from van Zeipel & Lindgren (1921). We observed eight of the 23 clump giants in this cluster’s instrumental CMD; all of the target-cluster giants in NGC 2099 are taken from the well-populated clump. The observed stars all had membership probabilities of greater than 75%, according to WEBDA.

NGC 2099 is a relatively unstudied cluster with few metallicity measurements. It is also the second cluster (after NGC 1245) to be observed by the STEPSS transiting planet search. Twarog et al. (1997) are some of the few to have studied NGC 2099. They use DDO photometry to derive $[\text{Fe}/\text{H}]=+0.089\pm 0.146$. Our value of $[\text{m}/\text{H}]=+0.05\pm 0.05$ is consistent with the metallicity cited by Twarog et al. (1997) to 0.2 sigma.

4.2.3. NGC 2324

We derive a metallicity for NGC 2324 of $[m/H] = -0.06 \pm 0.04$ from three measurements of four stars. The scatter in metallicity determinations among the stars observed in NGC 2324, 0.07 dex, is close to the expected level given the error in the method. Identifiers for these target-cluster stars are from Piatti et al. (2004). This cluster has a relatively well-defined clump; our target-cluster stars were selected from the seven giants in the clump. WEBDA reports very low membership probabilities for two of these stars; 0850 is given as 35% and 1006 is 11%. The third star, 1552, does not have a membership probability reported in WEBDA. These numbers are surprising, since our results have low scatter and the stars fall within the region of the clump in the CMD.

Friel et al. (2002) studied NGC 2324 with the spectrophotometric line index method used in this paper. They report a metallicity for NGC 2324 of $[Fe/H] = -0.15 \pm 0.16$. Others have also studied this cluster: Piatti et al. (2004) use their own reddening data with the Washington photometric data of Geisler et al. (1992) to derive a metallicity of $[Fe/H] = -0.31 \pm 0.04$. Geisler et al. (1992) themselves derive $[Fe/H] \sim -1$ for this cluster. Cameron (1985) uses UV excess methods to derive $[Fe/H] = -0.163$.

We report $[m/H] = -0.06 \pm 0.04$ for NGC 2324. Our derived metallicity is consistent with the Friel et al. (2002) value to 0.5 sigma and with the Piatti et al. (2004) value to 4.4 sigma.

4.2.4. NGC 2539

The metallicity of NGC 2539 is $[m/H] = -0.04 \pm 0.03$, derived from four stars. The standard deviation of the metallicity estimates of the cluster stars observed in NGC 2539 is 0.05 dex. We use the Lapasset et al. (2000) identifiers for the target-cluster stars in this cluster. Our instrumental CMD of NGC 2539 showed a small clump with only a few stars; we observed all four of these clump stars. WEBDA does not report membership probabilities for this cluster, although due to the low scatter in metallicities we believe all of our target-cluster stars to in fact be members of the cluster.

Clariá & Lapasset (1986) derive a metallicity of $[Fe/H] = +0.2$ from DDO data; they also derive a value of $[Fe/H] = -0.2 \pm 0.1$ from iron lines. Twarog et al. (1997) publish an $[Fe/H]$ of $+0.137 \pm 0.062$ determined from DDO photometry.

Our derived metallicity differs from that of Twarog et al. (1997) by 2.6 sigma. We agree with the Clariá & Lapasset (1986) metallicity derived from iron lines to 1.5 sigma.

4.2.5. NGC 2682

We report a metallicity of $[m/H] = -0.05 \pm 0.02$ for NGC 2682 from five measurements of four cluster stars. The scatter is about half what we expect given the error in the method, 0.04 dex. Fagerholm (1906) provides the identifications for the stars in this target-cluster. All of our target-cluster stars have greater than 93% probabilities of being cluster members, according to WEBDA. NGC 2682 has the most evolved giant branch of any of the target-clusters; in this cluster we selected four stars from the instrumental CMD that were located along the giant branch.

NGC 2682 (M67) is one of the oldest known open clusters in the Galaxy; it is also by far the most-studied cluster in our sample, with many more metallicity determinations than discussed here. Previous studies agree that NGC 2682 has an approximately solar metallicity. Cayrel de Strobel (1990) uses high-resolution spectroscopy to obtain a metallicity for NGC 2682 of $[Fe/H] = +0.039 \pm 0.09$. Hobbs & Thorburn (1991) use high-resolution spectroscopy of weak iron lines to find $[Fe/H] = -0.04 \pm 0.12$. Both Friel & Janes (1993) and Friel et al. (2002) derive the metallicity of this cluster from indices used in this paper; they obtain metallicities of $[Fe/H] = -0.09 \pm 0.07$ and $[Fe/H] = -0.15 \pm 0.05$, respectively. Burstein et al. (1986) use a moderate resolution iron index to derive a metallicity of $[Fe/H] = -0.1^{+0.12}_{-0.04}$. Cameron (1985) uses the cluster’s UV excess to derive $[Fe/H] = -0.029$. Twarog et al. (1997) use DDO photometry to find $[Fe/H] = +0.000 \pm 0.092$.

Our derived metallicity for NGC 2682 agrees well with most metallicities given in the literature. This metallicity agrees with Cayrel de Strobel (1990) to 0.96 sigma and with Hobbs & Thorburn (1991) to 0.1 sigma. Our determination agrees with other metallicities derived from spectrophotometric line index methods as well: we reproduce the Friel & Janes (1993) value to 0.5 sigma and the Friel et al. (2002) value to 1.8 sigma. We agree with the lower error of Burstein et al. (1986) to 1.1 sigma; we agree with Twarog et al. (1997) to 0.5 sigma.

4.2.6. NGC 6705

The metallicity of NGC 6705 is $[m/H] = +0.14 \pm 0.08$, derived from four stars. The stars have a scatter of 0.16 dex. We use the identifiers of McNamara et al. (1977) for NGC 6705. These stars all had membership probabilities in WEBDA of 98% or greater. This cluster has a very sparse instrumental CMD; we observed four of the six giants in the well-defined clump.

Cameron (1985) also studied NGC 6705. For this cluster they derive $[\text{Fe}/\text{H}] = +0.070$ with UV excess methods. Twarog et al. (1997) give $[\text{Fe}/\text{H}] = +0.136 \pm 0.086$, derived by shifting spectroscopic measurements made by Thogerson et al. (1993) onto a scale in common with other literature values. Thogerson et al. (1993) derive $[\text{Fe}/\text{H}] = +0.21 \pm 0.09$ using spectrophotometric line indices.

We derive a metallicity for NGC 6705 of $[\text{m}/\text{H}] = +0.14 \pm 0.08$. This agrees very well with previous estimates; it is within 0.03 sigma of the metallicity derived by Twarog et al. (1997), and agrees with Thogerson et al. (1993) to 0.6 sigma.

4.2.7. NGC 6819

NGC 6819 has a metallicity of $[\text{m}/\text{H}] = +0.07 \pm 0.12$. This cluster has the largest scatter in metallicity determinations among cluster stars in our sample (0.24 dex). It is possible that some of the stars in our sample are not in fact cluster members. Unfortunately, WEBDA does not report membership probabilities for any of our stars in NGC 6819. Furthermore, the four stars selected in this cluster lie slightly below the giant branch of this evolved cluster. This may also account for some of the scatter in the derived metallicities of these stars. The identifiers for this target-cluster are taken from Auner (1974).

NGC 6819 is another old open cluster that has been studied more than the younger clusters. The cluster’s metallicity is derived in two papers using the index method: both Friel & Janes (1993) and Thogerson et al. (1993) derive $[\text{Fe}/\text{H}] = +0.05 \pm 0.11$. Bragaglia et al. (2001) use high-resolution spectroscopy to measure metal lines in three red clump stars in NGC 6819; they derive a metallicity of $[\text{Fe}/\text{H}] = +0.09 \pm 0.03$. Twarog et al. (1997) give $[\text{Fe}/\text{H}] = +0.074 \pm 0.123$, again obtained by shifting spectroscopic measurements made by Friel & Janes (1993) and Thogerson et al. (1993) onto a scale in common with other literature values.

Our metallicity estimate for NGC 6819 is $[\text{m}/\text{H}] = +0.07 \pm 0.12$, in excellent agreement with existing literature values. We agree with Friel & Janes (1993) and Thogerson et al. (1993) to 0.12 sigma, with Twarog et al. (1997) to 0.02 sigma, and with Bragaglia et al. (2001) to 0.16 sigma.

5. Conclusions

We have derived metallicity estimates for seven Galactic open clusters. We use moderate-resolution spectroscopy to estimate metallicities of giants in these clusters, calibrating our

results with high-resolution metallicity determinations of field giants. We reproduce the high-resolution determinations to 0.08 dex. Our derived metallicities generally agree with those found in the literature; more importantly, we provide new metallicity estimates for several clusters that are not well studied.

This method is of interest because it requires little observing time, relatively small telescopes, and the results are arrived at quickly compared to more complicated methods (such as those used in Paper I). This method is also more robust than many photometric techniques, as it relies on quantitative spectroscopy and relative index measurements, not on the generally unpredictable photometricity of the night sky. We have demonstrated that it reproduces the metallicities of calibration stars of known metallicity well. The measured indices are easily reproducible on different telescopes and even, as evidenced by comparison of our indices to the published indices of Friel (1987), by different instruments and observers.

The metallicity estimates given here will allow for selection of open clusters in which to conduct future transiting extra-solar planet searches.

The authors wish to thank W. Dias for making an updated version of part of his open cluster catalog available to us prior to publication. We have made extensive use of the WEBDA database as well as the VizieR Service.

This work was supported by NASA grant NAGS-10678. A. Gould was supported by grant AST 02-01266 from the NSF.

REFERENCES

- Auner, G. 1974, *A&AS*, 13, 143
- Bragaglia, A., Carretta, E., Gratton, R. G., et al. 2001, *AJ*, 121, 327
- Burke, C. J., DePoy, D. L., Gaudi, B. S., Marshall, J. L., & Pogge, R. W. 2003, in *ASP Conf. Ser. 294, Scientific Frontiers in Research on Extrasolar Planets*, ed. D. Deming & S. Seager (San Francisco: ASP), 379
- Burke, C. J., Gaudi, B.S., DePoy, D. L., Pogge, R. W., & Pinsonneault, M. H. 2004, *AJ*, 127, 2382
- Burstein, D., Faber, S. M., Gaskell, C. M., & Krumm, N. 1984, *ApJ*, 287, 586
- Burstein, D., Faber, S. M., & Gonzalez, J. J. 1986 *AJ*, 91, 1130
- Cameron, I. M. 1985, *A&A*, 147, 39
- Cayrel de Strobel, G. 1990, *Soc. Astron. Italiana, Memorie*, 61, 613
- Cayrel de Strobel, G., Soubiran, C., Ralite, N. 2001, *A&A*, 373, 159
- Chincarini, G. 1964, *Mem. Soc. Astr. Italiana* 35, 133
- Clariá, J. J., & Lapasset, E. 1986, *ApJ*, 302, 656
- Cottrell, P. L., & Sneden, C. 1986, *A&A*, 161, 314
- Dias, W. S., Alessi, B. S., Moitinho, A., & Lépine, J. R. D. 2002, *A&A*, 389, 871
- de La Fuente Marcos, R., & de La Fuente Marcos, C. 2004, *New Astronomy*, 9, 475
- ESA 1997, *The Hipparcos and Tycho Catalogues*, ESA SP-1200
- Fagerholm, E. 1906, *Uppsala Dissertation*
- Friel, E. D. 1987, *AJ*, 93, 1388
- Friel, E. D. 1995, *ARA&A*, 33, 381
- Friel, E. D., & Janes, K. A. 1993, *A&A*, 267, 75
- Friel, E. D., Janes, K. A., Tavares, M., Scott, J., Katsanis, R., Lotz, J., Hong, L., & Miller, N. 2002, *ApJ*, 124, 2693

- Geisler, D., Clariá, J. J., Minnitt, D. 1992, *AJ*, 104, 1892
- Gratton, R. 2000, *ASP Conf. Ser.* 198, 225
- Gonzalez, G. 1997, *MNRAS*, 285, 403
- Gonzalez, G. & Laws, C. 2000, *AJ*, 119, 390
- Gould, A., Stutz, A., Frogel, J. A. 2001, *ApJ*, 547, 590
- Hobbs, L. M., & Thorburn, J. A. 1991, *AJ*, 102, 1070
- Janes, K., & Adler, D. 1982, *ApJS*, 49, 425
- Janes, K. A., & Phelps, R. L. 1994, *AJ*, 108, 1773
- Kiss, L. L., Szabó, Gy. M., Furész, G., Sárneczky, K., & Csák, B. 2001, *A&A*, 376, 561
- Kyeong, J.-M., Byun, Y.-I., & Sung, E.-C. 2001, *J. Korean Astron. Soc.*, 34, 143
- Lapasset, E., Clariá, J. J., & Mermiliod, J.C. 2000, *A&A*, 361, 945
- Lynga, G. 1987, *Catalogue of Open Cluster Data* (5th ed.; Lund: Lund Obs.)
- McNamara, B. J., et al. 1977, *A&AS*, 27, 117
- Mermiliod, J.-C., Huestamendia, G., del Rio, G., Mayor, M. 1996, *A&A*, 307, 80
- Montgomery, K. A., Marschall, L. A., & Janes, K. A. 1993, *AJ*, 106, 181
- Perryman, M. A. C., et al. 1997, *A&A*, 323, L49
- Piatti, A. E., Clariá, J. J., & Ahumada, A. V. 2004, *A&A*, 418, 979
- Rosvick, J. M., & Vandenberg, D. A. 1998, *AJ*, 115, 1516
- Santos, N. C., Israelian, G., & Mayor, M. 2000, *A&A*, 363, 228
- Stetson, P. B. 2000, *PASP*, 112, 925
- Strader, J., & Brodie, J. P. astro-ph/0407001
- Strom, K.M. 1977, Kitt Peak National Observatory Memorandum, “Standard Stars for Intensified Image Dissector Scanner Observations”.
- Sung, H., Bessell, M. S., Lee, H.-W., Kang, Y. H., & Lee, S.-W. 1999, *MNRAS*, 310, 982

Thogersen, E. N., Friel, E. D., & Fallon, B. V. 1993, *PASP*, 105, 1253

Twarog, B. A., Ashman, K. M., Anthony-Twarog, B. J. 1997, *AJ*, 114, 2556

van Zeipel, H., & Lindgren, J. 1921, *Kungl. Sv. Vetensk. Handlingar* 61 no

Wee, S.-O., & Lee, M. G. 1996, *J. Korean Astron. Soc.*, 29, 181

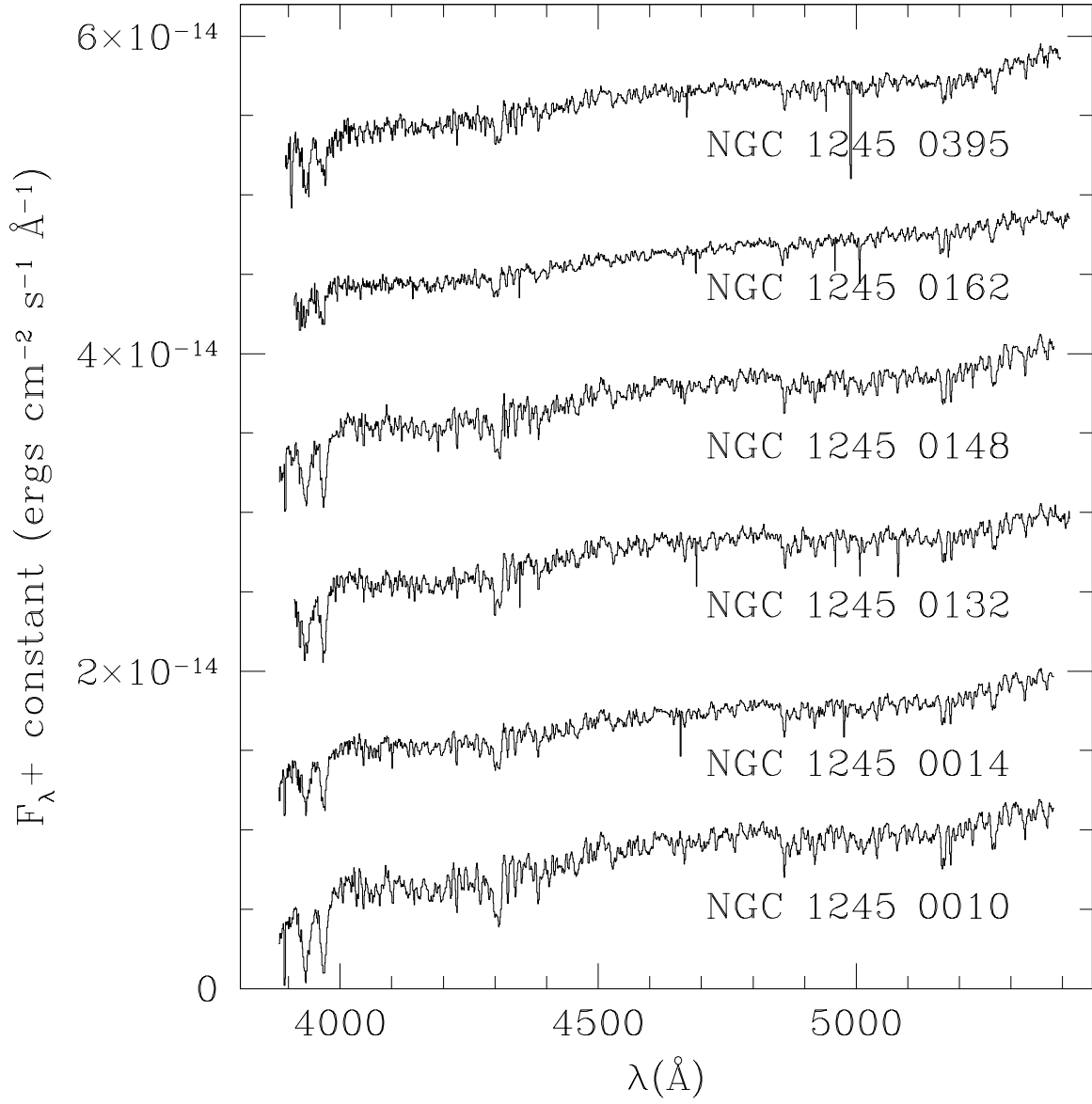


Fig. 1.— Spectra of all target-cluster stars observed in the cluster NGC 1245. Each spectrum includes an additive constant for display purposes.

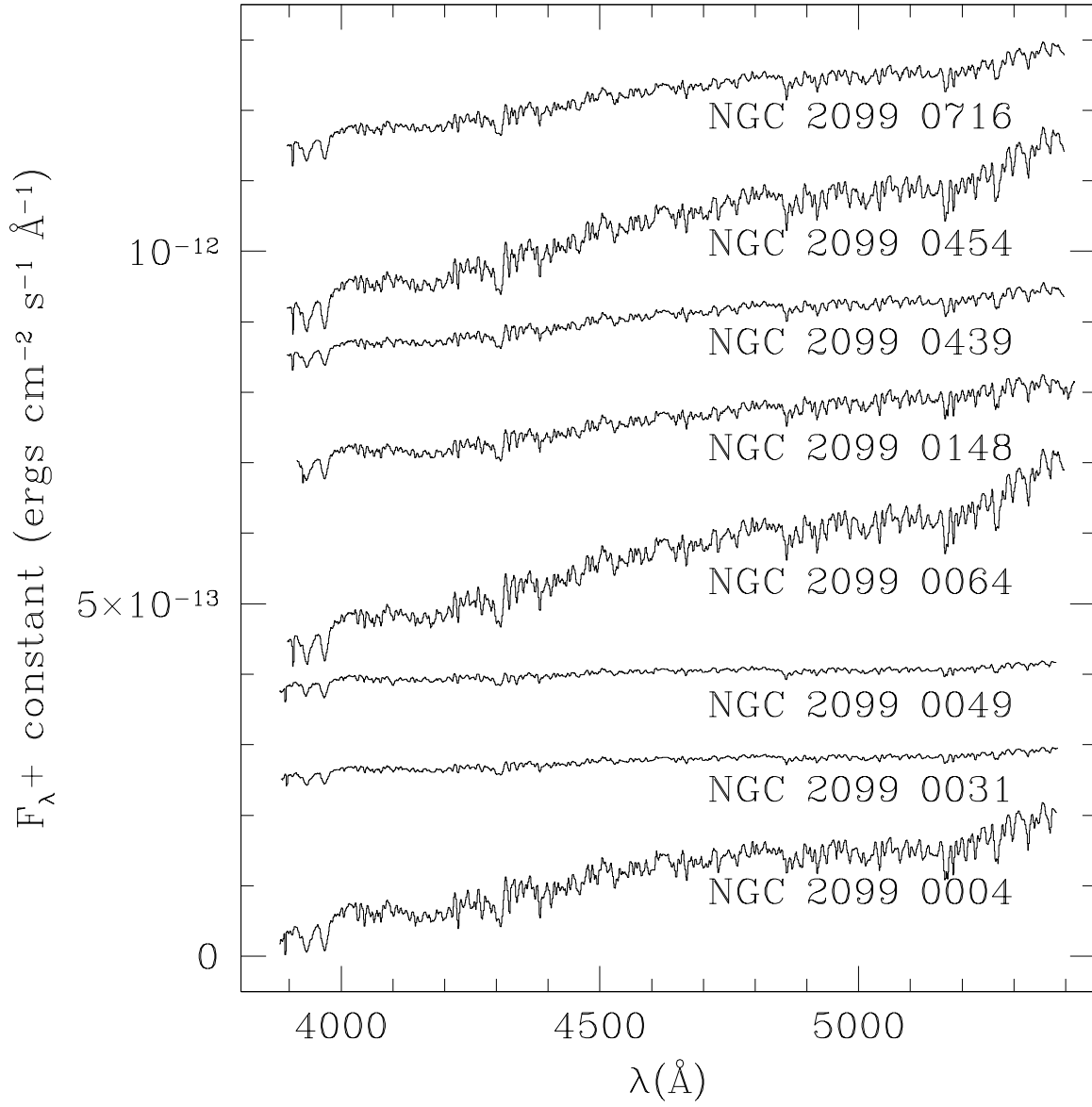


Fig. 2.— Same as Figure 1, but for the cluster NGC 2099.

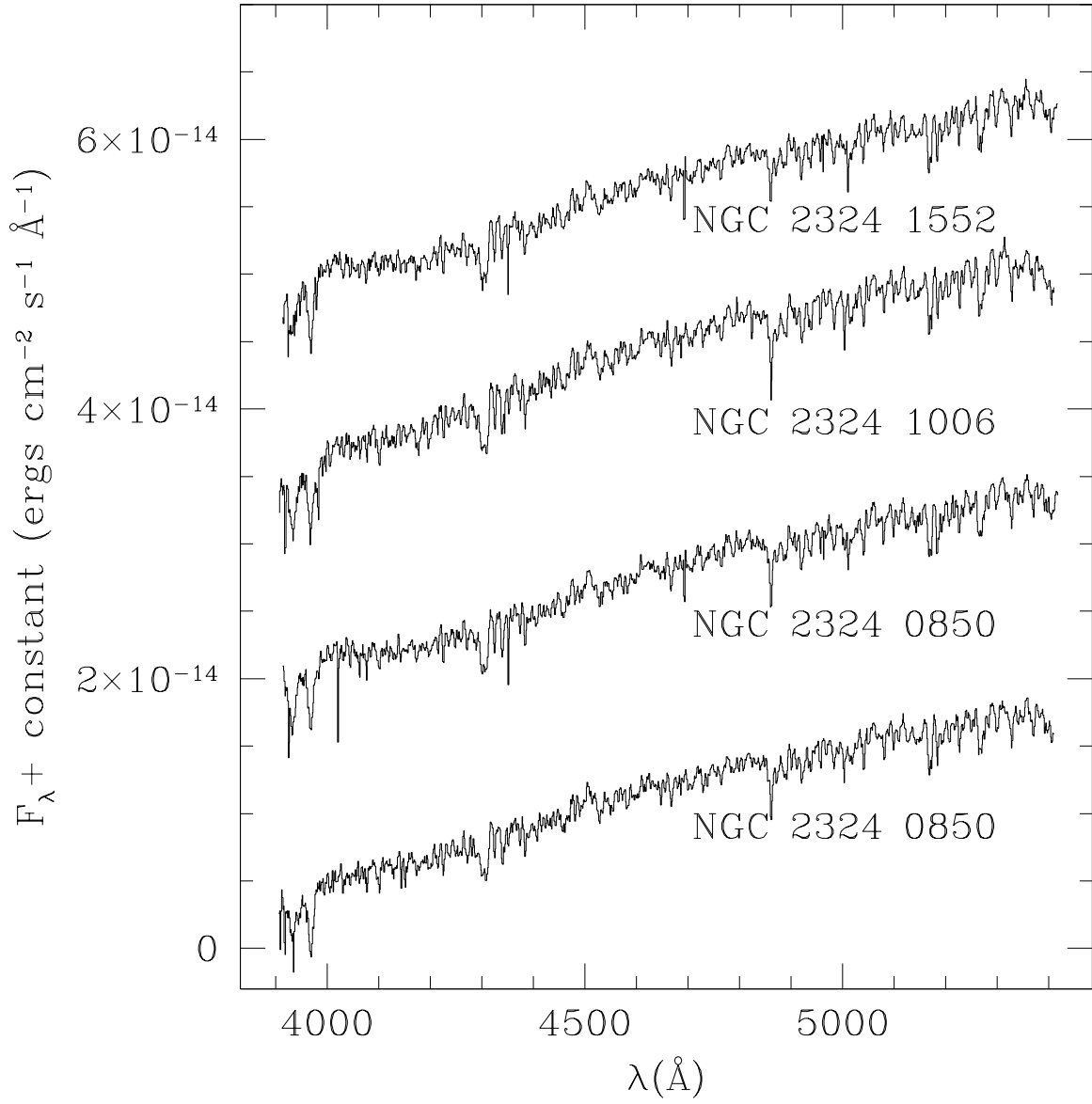


Fig. 3.— Same as Figure 1, but for the cluster NGC 2324.

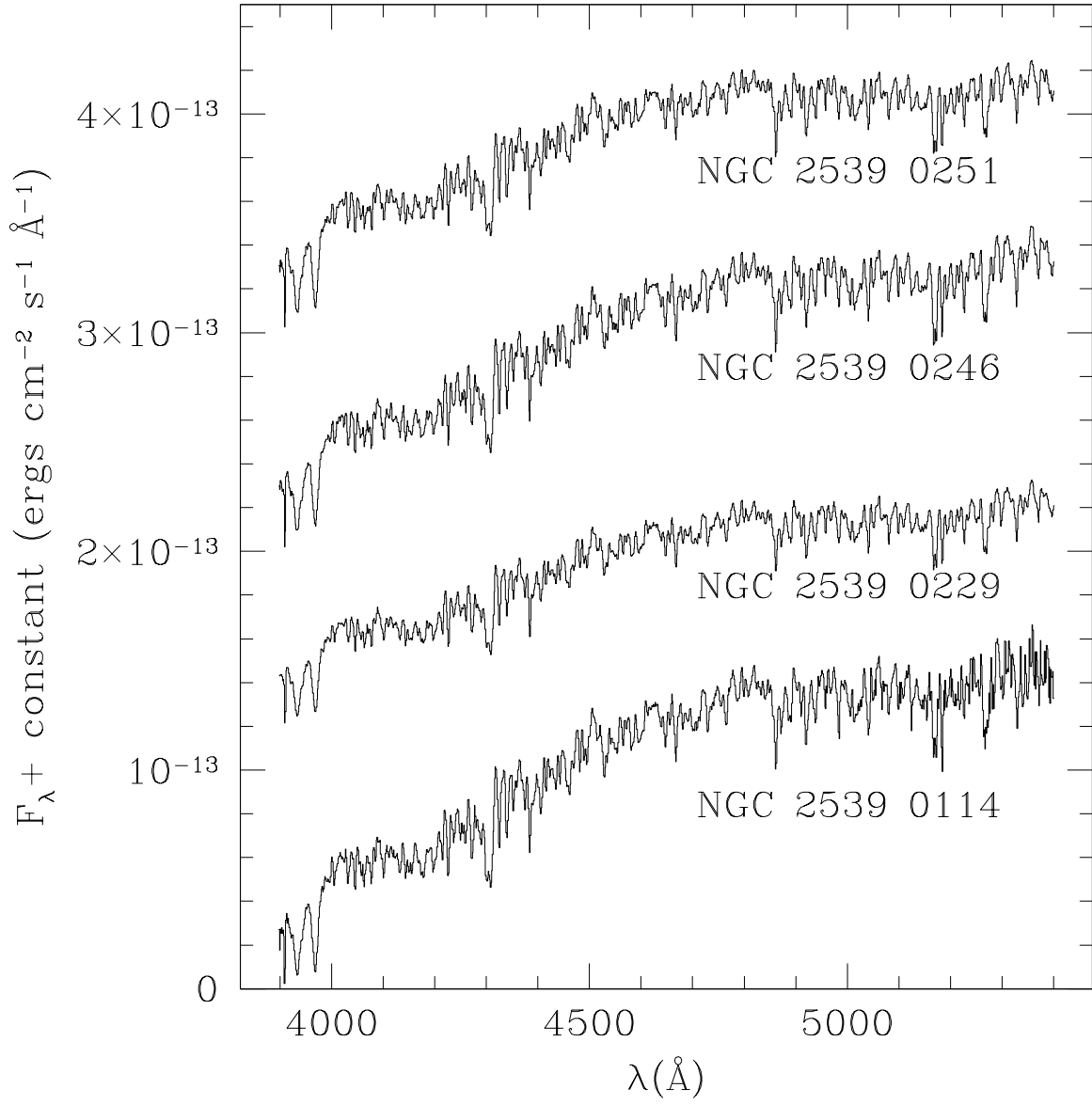


Fig. 4.— Same as Figure 1, but for the cluster NGC 2539.

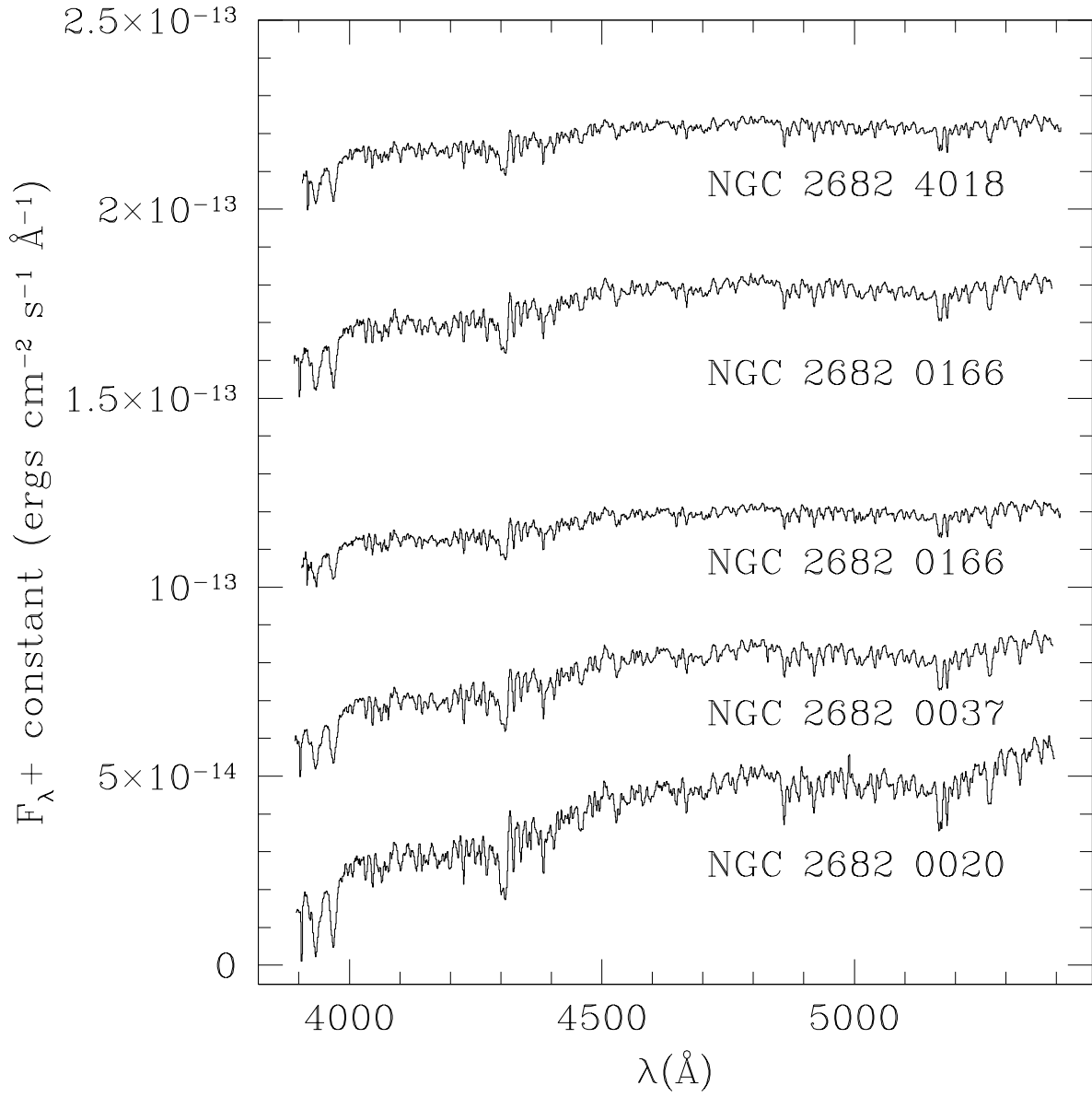


Fig. 5.— Same as Figure 1, but for the cluster NGC 2682.

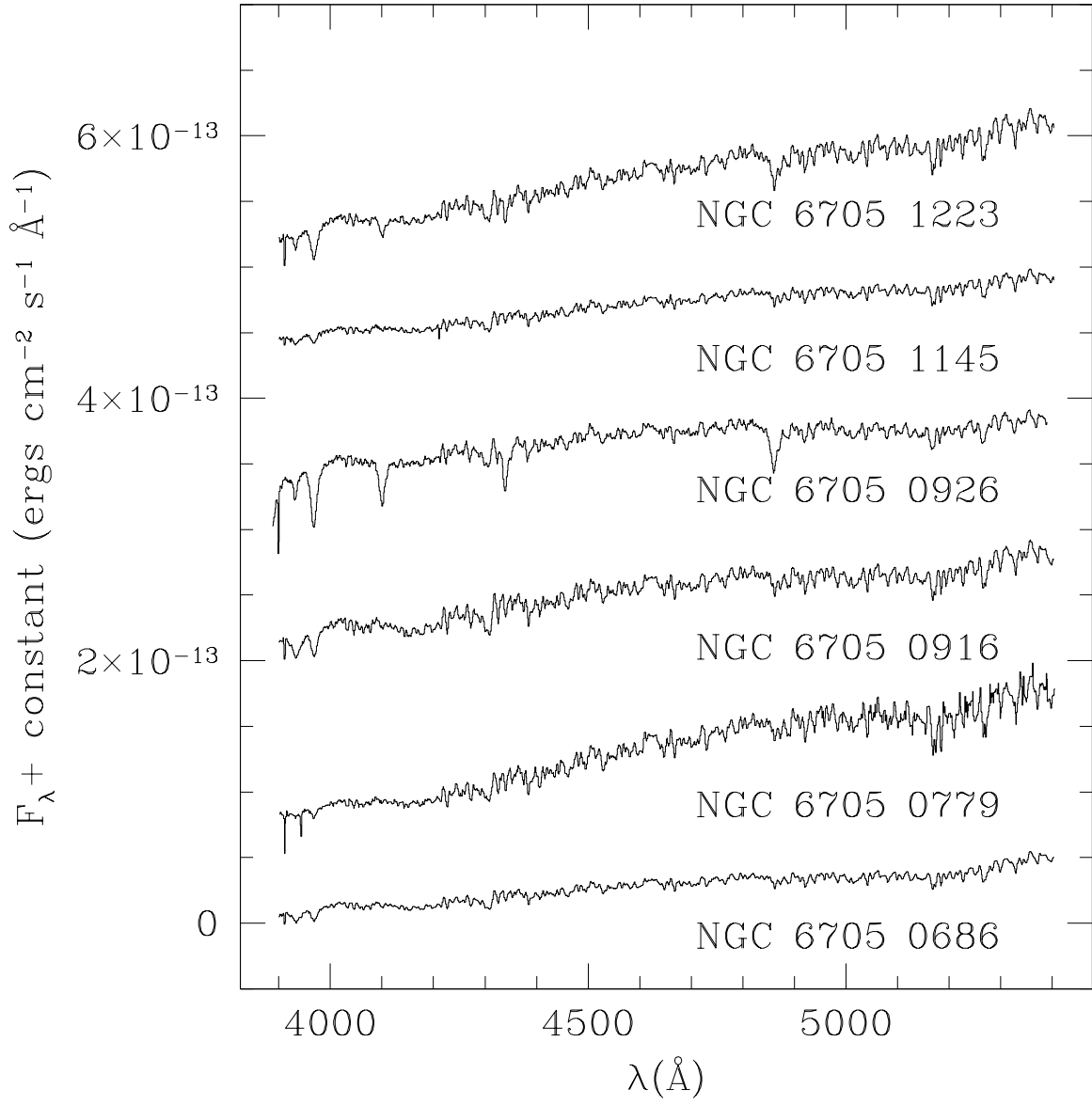


Fig. 6.— Same as Figure 1, but for the cluster NGC 6705.

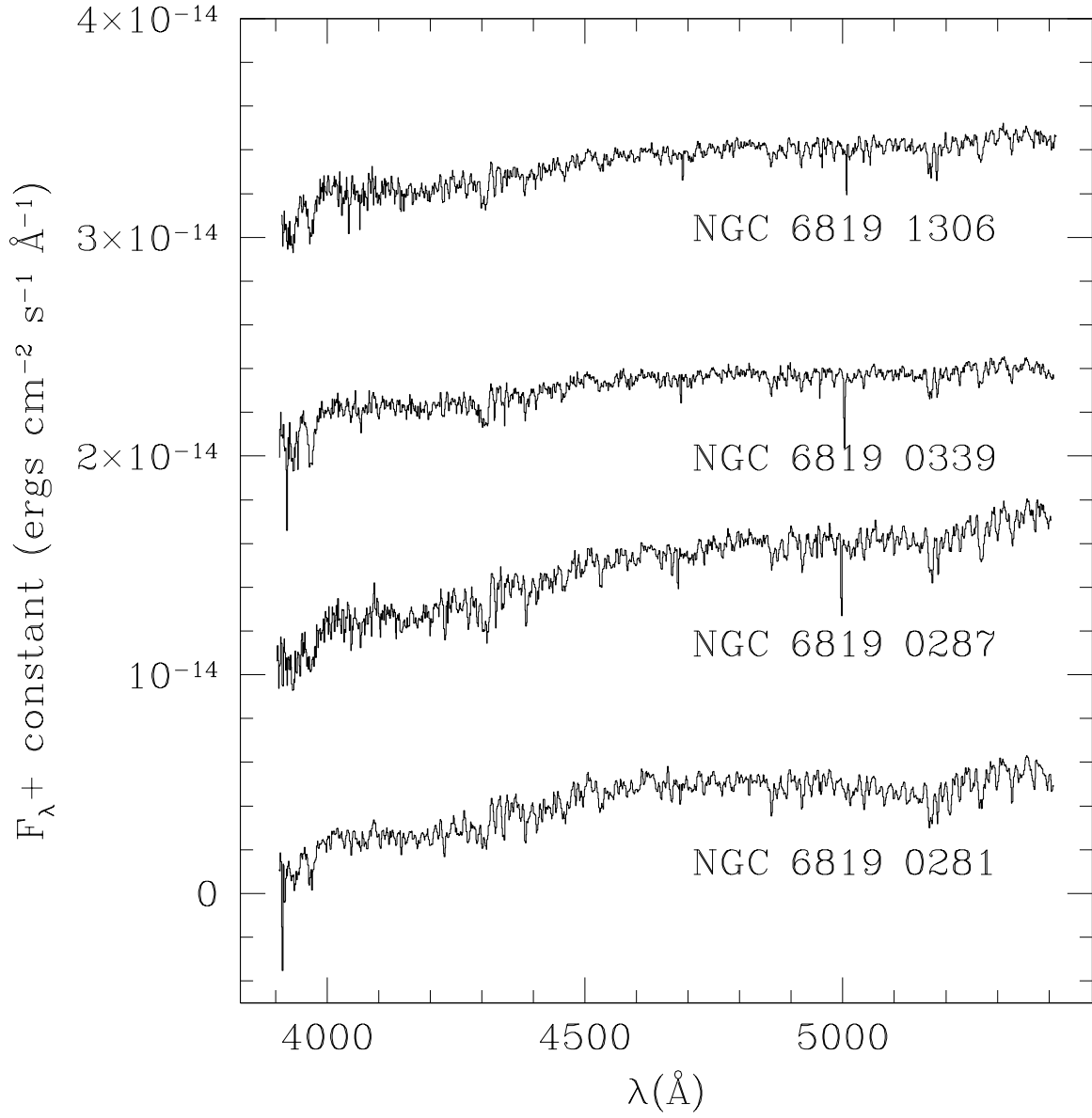


Fig. 7.— Same as Figure 1, but for the cluster NGC 6819.

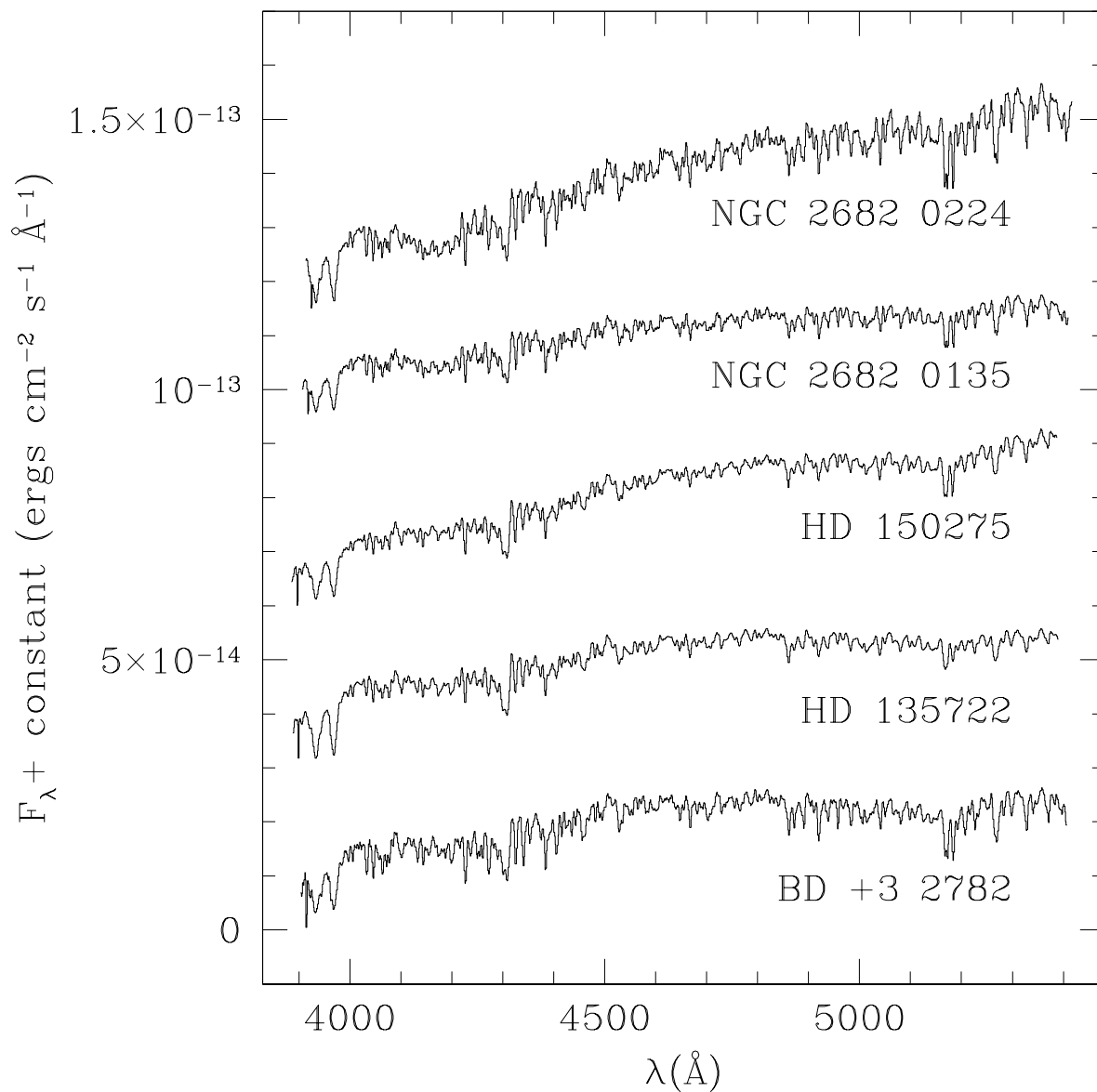


Fig. 8.— Spectra of selected calibration field red giants in a range of colors. Shown are BD +3 2782 ($B - V = 0.9$), HD 135722 ($B - V = 0.95$), HD 150275 ($B - V = 1.0$), NGC 2682 0135 ($(B - V)_0 = 1.06$), and NGC 2682 0224 ($(B - V)_0 = 1.1$). The spectra are normalized to BD +3 2782 at 4500 Å, and include an additive constant for display purposes.

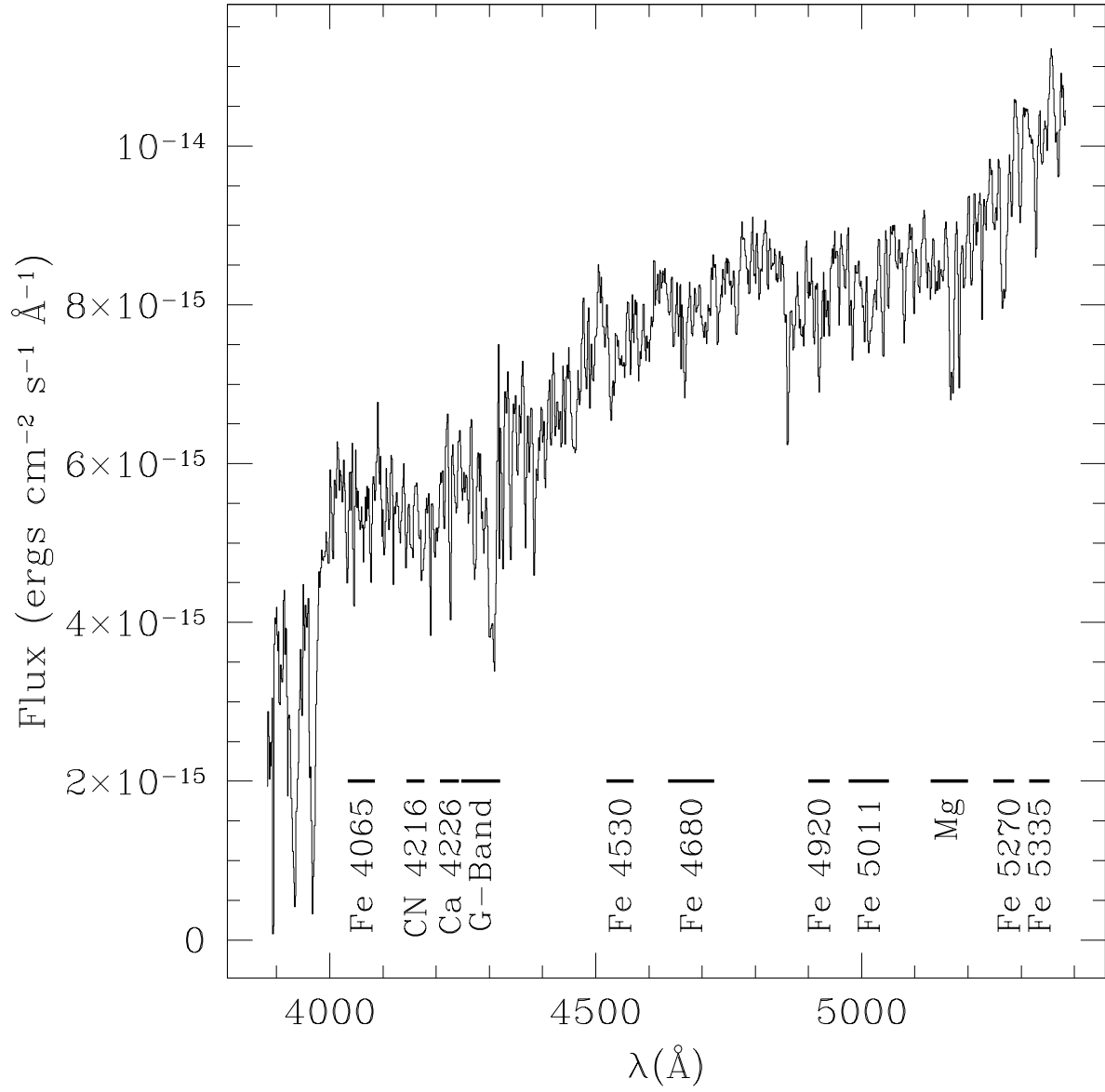


Fig. 9.— An example spectrum (of the target-cluster star NGC 1245 0148) showing the central bandpasses and widths of indices measured in this paper.

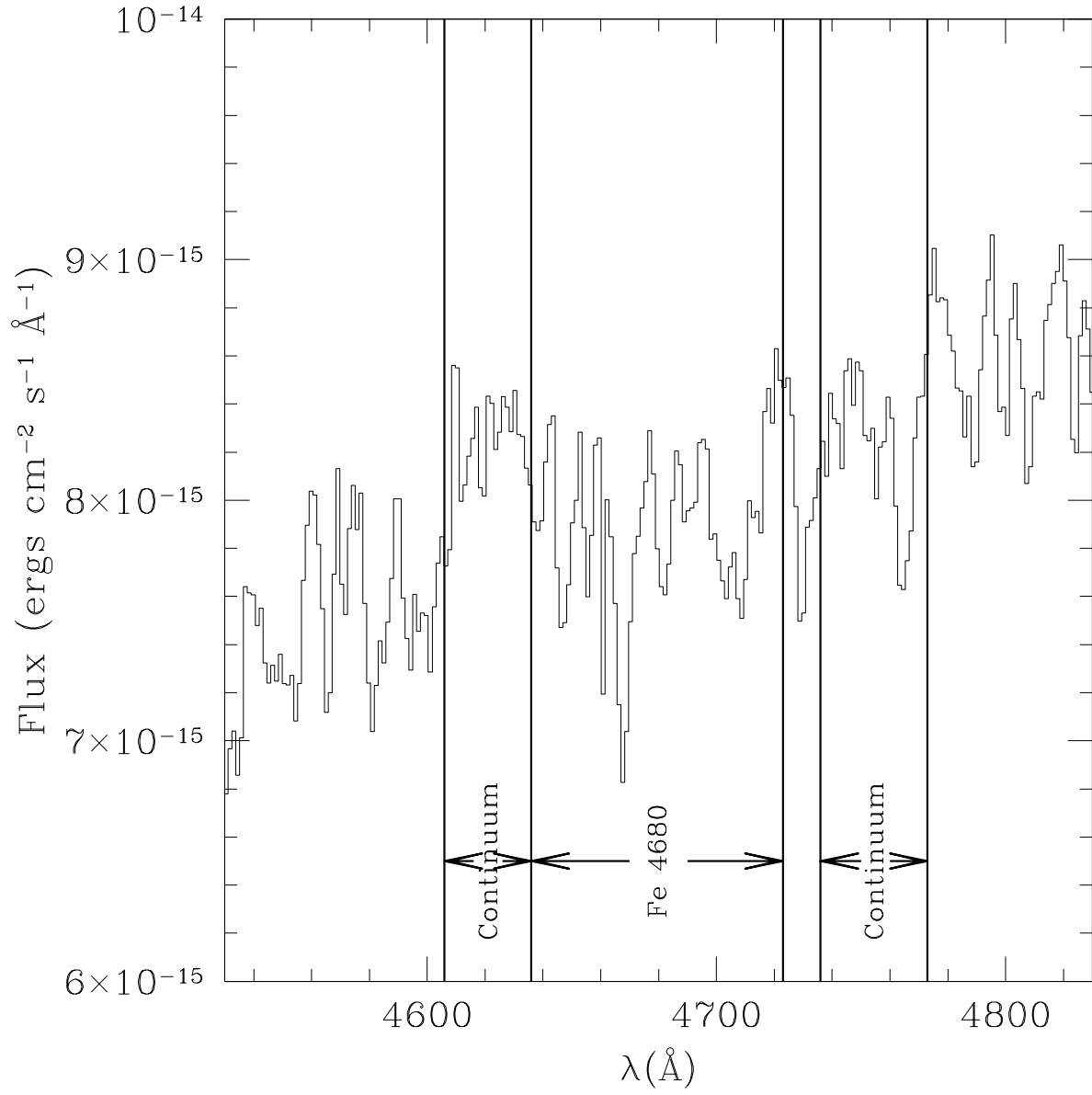


Fig. 10.— An enlarged portion of the spectrum shown in Figure 9, detailing the placement of one index (Fe4680) and its flanking continuum bandpasses

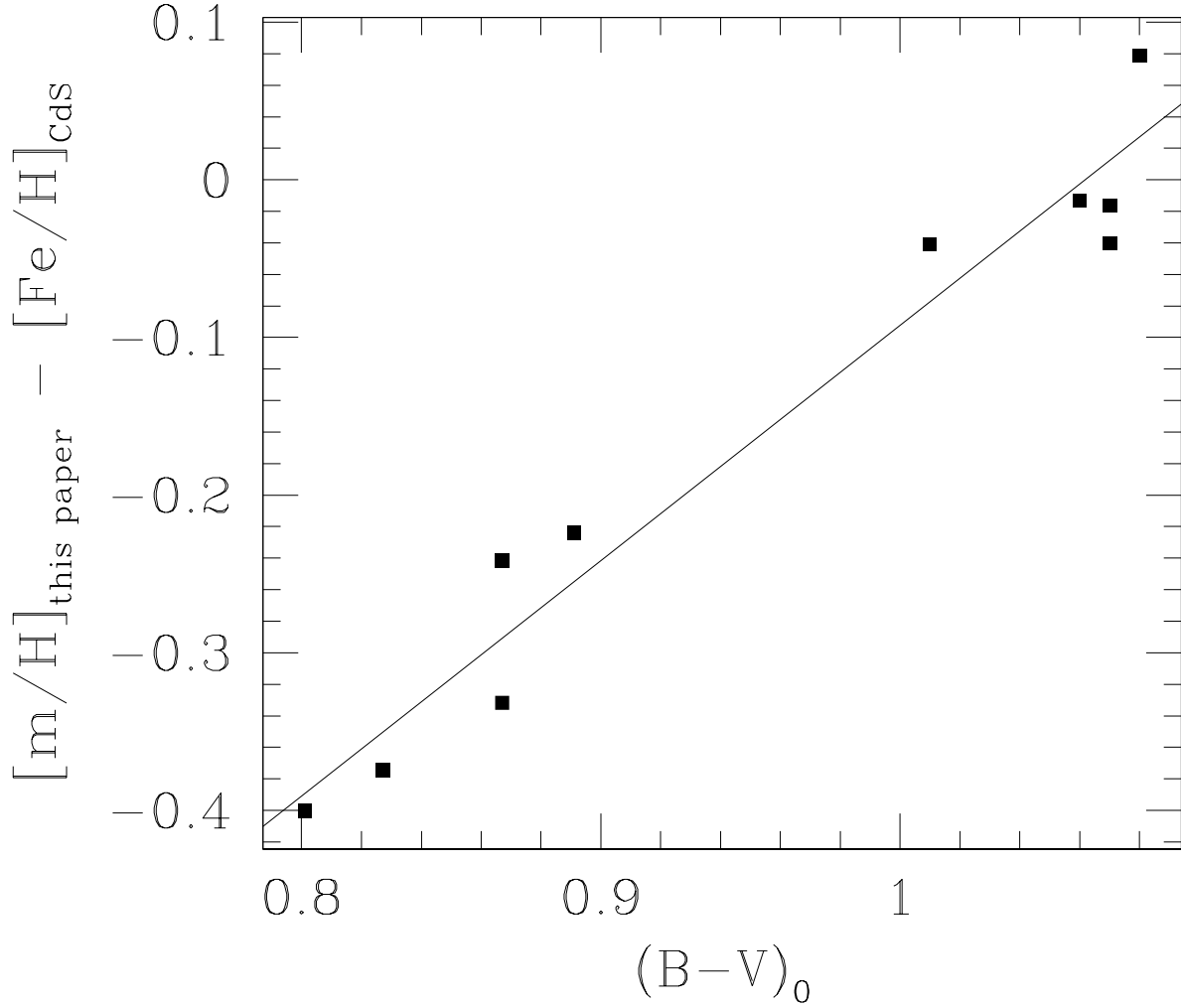


Fig. 11.— Derivation of the color correction term applied to the target-cluster stars to determine their final metallicities.

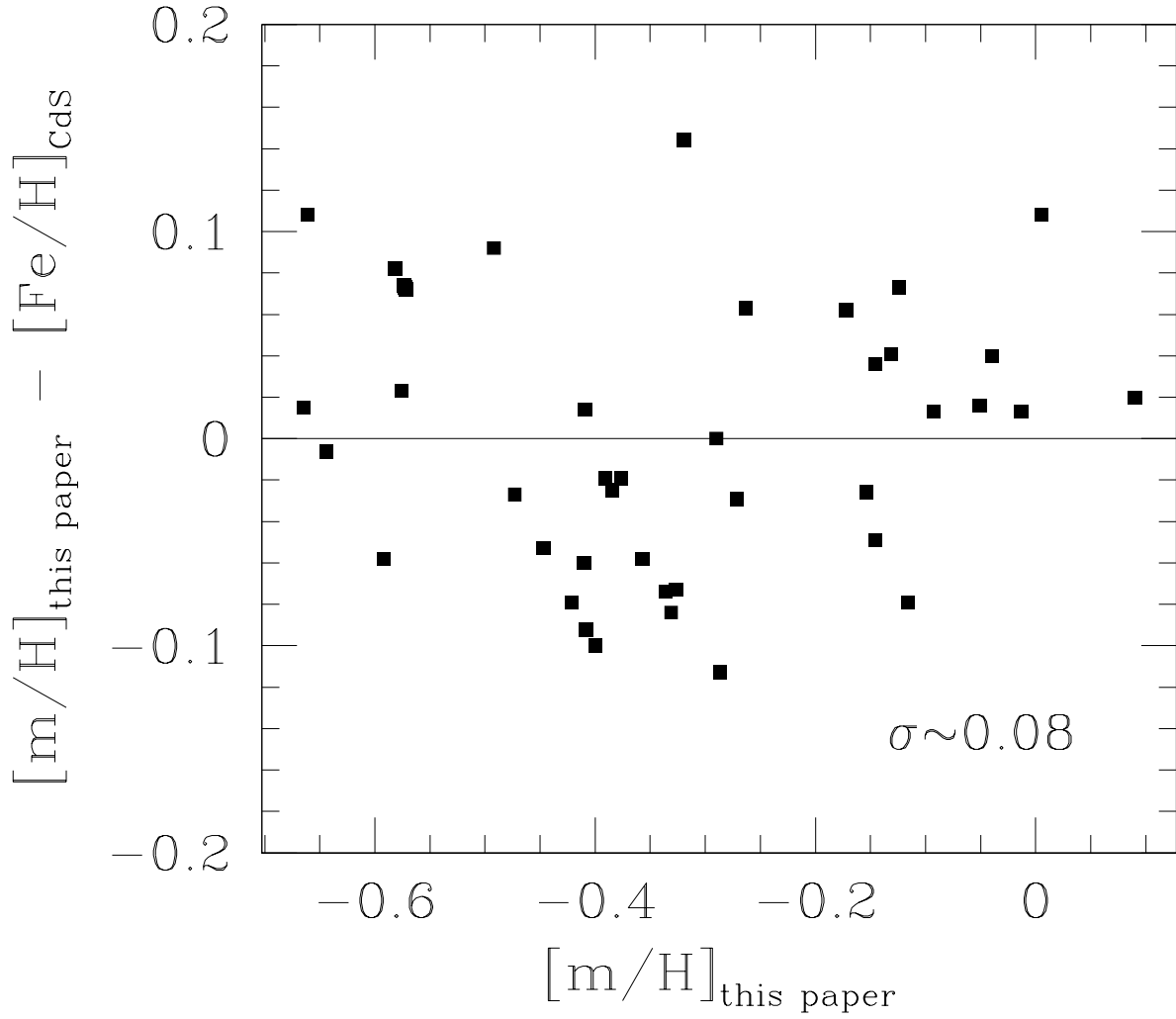


Fig. 12.— Comparison of metallicities derived here with those of Cayrel de Strobel et al. (2001). The scatter is ~ 0.08 dex.

Table 1. Indices Measured

Index	Central Bandpass	Continuum Bandpass	Species Measured
Fe4065	4033.50 - 4085.00	4006.00 - 4038.00 4085.00 - 4115.00	Fe I, Mn I, Sr II
CN4216	4144.00 - 4177.75	4082.00 - 4118.25 4246.00 - 4284.75	CN ($B^2\Sigma^+ - X^2\Sigma^+$)
Ca4226	4207.00 - 4245.00	4115.00 - 4165.00 4320.00 - 4370.00	Ca I
G-band	4245.00 - 4320.00	4120.00 - 4200.00 4425.00 - 4520.00	CH, Fe I
Fe4530	4520.00 - 4571.25	4498.75 - 4520.00 4606.00 - 4636.00	Fe I, Ti I, Ti II
Fe4680	4636.00 - 4723.00	4606.00 - 4636.00 4736.00 - 4773.00	Fe I, Cr I, Ni I, Mg I
Fe4920	4900.00 - 4940.00	4796.00 - 4841.00 4935.00 - 4975.00	Fe I
Fe5011	4976.00 - 5051.00	4935.00 - 4975.00 5051.00 - 5096.00	Fe I, Ti I, Fe II, Ni I
Mg	5130.00 - 5200.00	4935.00 - 4975.00 5303.00 - 5367.00	Mg b + MbH
Fe5270	5248.00 - 5286.75	5220.00 - 5250.00 5288.00 - 5322.00	Fe I, Ca I
Fe5335	5314.75 - 5353.50	5307.25 - 5317.25 5356.00 - 5364.75	Fe I, Cr I

Table 2. Metallicity indices for calibration stars

Star Name	Date Observed	(B-V) ₀ ^a	[Fe/H] ^b	Ca4226	CN4216	Fe4065	Fe4530	Fe4680	Fe4920	Fe5011	Fe5270	Fe5335	Gband	Mg
α UMa	Jan 31	1.061	-0.19	0.783	0.982	0.822	0.883	0.811	0.838	0.818	0.825	0.828	0.914	0.889
α UMa	Mar 25	1.061	-0.19	0.793	0.996	0.819	0.886	0.819	0.816	0.806	0.829	0.833	0.969	0.936
BD +3 2782	Mar 29	1.092	-2.0233	0.863	0.785	0.882	0.835	0.812	0.833	0.794	0.850	0.851	1.040	0.964
β Gem	Mar 31	0.991	-0.0517	0.830	0.960	0.849	0.862	0.823	0.807	0.804	0.837	0.841	0.975	0.862
ϵ Vir	Jan 31	0.934	0.148	0.777	0.954	0.832	0.855	0.819	0.847	0.819	0.833	0.824	0.900	0.887
ϵ Vir	Mar 29	0.934	0.148	0.791	0.958	0.827	0.864	0.820	0.829	0.810	0.832	0.831	0.916	0.865
ϵ Vir	Mar 31	0.934	0.148	0.801	0.960	0.830	0.863	0.820	0.810	0.807	0.827	0.828	0.927	0.845
HD 108225	Mar 22	0.955	-0.11	0.806	0.936	0.830	0.853	0.819	0.818	0.805	0.835	0.836	0.930	0.875
HD 108225	Mar 31	0.955	-0.11	0.814	0.933	0.841	0.857	0.822	0.816	0.805	0.831	0.829	0.949	0.893
HD 111028	Jan 31	0.989	-0.4	0.817	0.849	0.844	0.848	0.813	0.831	0.800	0.834	0.828	1.008	0.917
HD 111028	Mar 23	0.989	-0.4	0.822	0.860	0.846	0.846	0.812	0.812	0.789	0.834	0.842	1.004	0.923
HD 111028	Mar 24	0.989	-0.4	0.819	0.859	0.838	0.846	0.813	0.824	0.794	0.833	0.838	0.997	0.938
HD 117876	Jan 31	0.969	-0.5	0.790	0.839	0.815	0.846	0.791	0.821	0.797	0.816	0.820	0.969	0.873
HD 117876	Mar 22	0.969	-0.5	0.801	0.851	0.811	0.850	0.795	0.800	0.793	0.816	0.818	0.975	0.880
HD 117876	Mar 24	0.969	-0.5	0.796	0.849	0.813	0.848	0.792	0.814	0.794	0.813	0.815	0.972	0.884
HD 122563	Mar 22	0.853	-2.683	0.770	0.752	0.737	0.779	0.753	0.768	0.749	0.760	0.764	0.862	0.732
HD 122563	Mar 31	0.853	-2.683	0.786	0.756	0.744	0.785	0.756	0.766	0.748	0.762	0.765	0.881	0.763
HD 129312	Mar 23	0.992	-0.31	0.785	0.981	0.826	0.867	0.819	0.818	0.812	0.834	0.831	0.910	0.908
HD 130952	Jan 31	0.988	-0.395	0.799	0.861	0.832	0.857	0.802	0.852	0.811	0.809	0.825	1.034	0.917
HD 130952	Mar 24	0.988	-0.395	0.798	0.862	0.816	0.849	0.805	0.809	0.793	0.821	0.838	1.005	0.892
HD 135722	Mar 24	0.961	-0.47	0.799	0.829	0.824	0.851	0.795	0.816	0.797	0.812	0.813	0.991	0.863
HD 138905	Mar 24	1.007	-0.41	0.801	0.874	0.831	0.853	0.797	0.819	0.795	0.818	0.821	0.992	0.877
HD 138905	Mar 31	1.007	-0.41	0.828	0.886	0.831	0.860	0.796	0.804	0.794	0.821	0.821	1.022	0.844
HD 150275	Mar 24	0.995	-0.5	0.818	0.791	0.813	0.850	0.787	0.801	0.790	0.809	0.810	1.043	0.908
HD 150275	Mar 31	0.995	-0.5	0.835	0.802	0.818	0.859	0.791	0.782	0.786	0.816	0.820	1.077	0.853
HD 168322	Mar 24	0.977	-0.4	0.800	0.815	0.810	0.848	0.799	0.814	0.798	0.809	0.811	1.012	0.887
HD 198149	Apr 01	0.912	-0.41	0.810	0.833	0.832	0.840	0.804	0.818	0.787	0.820	0.822	1.011	0.890
HD 199191	Apr 01	0.960	-0.7	0.806	0.776	0.810	0.835	0.786	0.801	0.783	0.805	0.808	1.028	0.882
HD 25975	Mar 30	0.943	-0.2	0.823	0.895	0.844	0.847	0.820	0.834	0.798	0.842	0.840	0.989	0.991
HD 27371	Mar 24	0.981	0.1128	0.788	1.021	0.832	0.859	0.830	0.828	0.811	0.835	0.837	0.914	0.869
HD 27971	Mar 31	0.986	-0.08	0.813	0.971	0.842	0.863	0.827	0.818	0.807	0.832	0.835	0.957	0.860
HD 37160	Mar 30	0.951	-0.5533	0.816	0.792	0.811	0.834	0.770	0.816	0.779	0.814	0.820	1.052	0.891
HD 37160	Mar 31	0.951	-0.5533	0.823	0.793	0.814	0.844	0.790	0.785	0.781	0.812	0.817	1.071	0.856
HD 40460	Mar 30	1.022	-0.5	0.814	0.902	0.834	0.855	0.810	0.818	0.793	0.830	0.836	1.002	0.928
HD 41636	Mar 30	1.044	-0.3	0.801	0.914	0.825	0.845	0.814	0.824	0.798	0.830	0.829	0.990	0.975

Table 2—Continued

Star Name	Date Observed	(B-V) ₀ ^a	[Fe/H] ^b	Ca4226	CN4216	Fe4065	Fe4530	Fe4680	Fe4920	Fe5011	Fe5270	Fe5335	Gband	Mg
HD 43039	Mar 30	1.021	-0.415	0.819	0.886	0.831	0.850	0.804	0.819	0.796	0.829	0.831	1.006	0.937
HD 43039	Mar 31	1.021	-0.415	0.821	0.887	0.831	0.860	0.809	0.802	0.796	0.824	0.829	1.025	0.883
HD 46480	Jan 31	0.899	-0.5	0.784	0.759	0.810	0.832	0.784	0.832	0.792	0.799	0.807	1.003	0.932
HD 46480	Mar 31	0.899	-0.5	0.817	0.776	0.813	0.840	0.792	0.791	0.782	0.803	0.808	1.051	0.863
HD 62345	Mar 29	0.932	-0.18	0.789	0.947	0.828	0.855	0.813	0.824	0.804	0.829	0.828	0.931	0.867
HD 63410	Jan 31	0.961	-0.5	0.787	0.842	0.815	0.849	0.803	0.829	0.805	0.813	0.814	0.988	0.881
HD 63410	Mar 30	0.961	-0.5	0.806	0.851	0.816	0.840	0.797	0.820	0.790	0.822	0.824	1.003	0.903
HD 73710	Mar 31	1.020	0.11	0.810	1.065	0.843	0.887	0.841	0.811	0.812	0.841	0.845	0.932	0.866
HD 81192	Jan 31	0.933	-0.65	0.795	0.739	0.804	0.834	0.777	0.820	0.787	0.802	0.795	1.023	0.866
HD 81192	Mar 23	0.933	-0.65	0.803	0.751	0.802	0.837	0.778	0.795	0.781	0.811	0.812	1.031	0.913
HD 81192	Mar 23	0.933	-0.65	0.813	0.752	0.799	0.832	0.798	0.770	0.788	0.774	0.773	1.044	0.487
HD 85773	Mar 29	1.078	-2.31	0.773	0.807	0.762	0.797	0.764	0.778	0.757	0.777	0.778	0.904	0.771
HD 88609	Mar 23	0.894	-2.845	0.769	0.768	0.760	0.778	0.749	0.760	0.746	0.765	0.762	0.847	0.777
HD 91612	Mar 23	0.921	-0.175	0.795	0.851	0.826	0.850	0.802	0.812	0.798	0.818	0.813	0.958	0.825
HD 96436	Mar 23	0.955	-0.5	0.801	0.812	0.814	0.841	0.796	0.803	0.786	0.819	0.828	1.021	0.906
NGC 2682 0135	Mar 30	1.01	-0.09	0.829	0.966	0.847	0.867	0.823	0.818	0.797	0.840	0.848	0.962	0.906
NGC 2682 0141	Mar 30	1.06	0.0	0.814	1.009	0.847	0.863	0.830	0.816	0.804	0.839	0.839	0.942	0.889
NGC 2682 0164	Mar 31	1.07	0.0	0.837	1.032	0.853	0.874	0.828	0.801	0.806	0.839	0.845	1.002	0.885
NGC 2682 0224	Mar 31	1.08	-0.195	0.858	1.064	0.839	0.878	0.816	0.802	0.804	0.839	0.850	0.948	0.898
NGC 2682 0084	Mar 30	1.06	-0.035	0.814	0.998	0.845	0.871	0.827	0.816	0.803	0.835	0.845	0.960	0.877
o Vir	Mar 29	0.967	-0.29	0.783	0.849	0.834	0.851	0.802	0.817	0.789	0.807	0.808	0.999	0.839

^aColors taken from the Hipparcos Catalog (ESA 1997)^bMetallicities derived from Cayrel de Strobel et al. (2001), as described in §3

Table 3. Metallicity indices for target-cluster stars

Star Name ^a	Date Observed	(B-V) ₀ ^b	Ca4226	CN4216	Fe4065	Fe4530	Fe4680	Fe4920	Fe5011	Fe5270	Fe5335	Gband	Mg
NGC 1245 0010	Jan 31	0.878	0.779	0.836	0.829	0.851	0.799	0.829	0.809	0.816	0.811	0.959	0.859
NGC 1245 0014	Jan 31	0.914	0.778	0.814	0.825	0.842	0.804	0.826	0.815	0.811	0.807	0.962	0.874
NGC 1245 0132	Mar 30	0.899	0.819	0.852	0.819	0.845	0.805	0.809	0.794	0.821	0.818	0.980	0.879
NGC 1245 0148	Jan 31	0.918	0.768	0.851	0.805	0.849	0.800	0.833	0.812	0.818	0.813	0.956	0.881
NGC 1245 0162	Mar 31	0.897	0.814	0.874	0.777	0.822	0.800	0.790	0.798	0.783	0.756	0.973	0.834
NGC 1245 0395	Mar 24	0.896	0.773	0.849	0.816	0.835	0.808	0.822	0.838	0.822	0.810	0.962	0.893
NGC 2099 0004	Jan 31	0.88	0.832	1.051	0.864	0.890	0.830	0.832	0.823	0.845	0.843	0.960	0.954
NGC 2099 0031	Jan 31	0.90	0.779	0.923	0.831	0.858	0.810	0.852	0.820	0.821	0.809	0.934	0.890
NGC 2099 0049	Jan 31	0.90	0.717	0.814	0.765	0.839	0.796	0.835	0.812	0.809	0.797	0.895	0.879
NGC 2099 0064	Mar 25	0.96	0.810	1.021	0.841	0.875	0.818	0.819	0.815	0.840	0.831	0.969	0.939
NGC 2099 0148	Mar 31	0.98	0.806	1.009	0.834	0.878	0.822	0.805	0.812	0.829	0.822	0.960	0.847
NGC 2099 0439	Mar 25	0.90	0.795	0.931	0.826	0.862	0.809	0.814	0.801	0.827	0.825	0.954	0.859
NGC 2099 0454	Mar 25	0.94	0.786	1.009	0.826	0.878	0.820	0.818	0.813	0.839	0.828	0.965	0.921
NGC 2099 0716	Mar 25	0.87	0.789	0.913	0.815	0.859	0.803	0.816	0.801	0.826	0.816	0.959	0.890
NGC 2324 0850	Mar 30	0.75	0.791	0.840	0.768	0.856	0.789	0.792	0.799	0.806	0.809	0.957	0.782
NGC 2324 0850	Mar 31	0.75	0.774	0.813	0.763	0.851	0.798	0.794	0.798	0.809	0.813	0.965	0.799
NGC 2324 1006	Mar 30	0.77	0.754	0.826	0.763	0.847	0.792	0.794	0.798	0.821	0.807	0.941	0.791
NGC 2324 1552	Mar 31	0.79	0.800	0.858	0.812	0.862	0.801	0.783	0.799	0.810	0.807	0.999	0.808
NGC 2539 0114	Mar 29	0.906	0.813	0.933	0.815	0.857	0.812	0.819	0.809	0.845	0.832	0.970	0.846
NGC 2539 0229	Mar 29	0.926	0.804	0.957	0.828	0.857	0.810	0.822	0.804	0.832	0.830	0.955	0.862
NGC 2539 0246	Mar 29	0.899	0.809	0.927	0.829	0.859	0.812	0.821	0.805	0.831	0.831	0.952	0.866
NGC 2539 0251	Mar 29	0.903	0.800	0.907	0.815	0.851	0.803	0.823	0.800	0.825	0.829	0.945	0.862
NGC 2682 0020	Mar 25	0.801	0.794	0.786	0.828	0.829	0.802	0.822	0.779	0.823	0.819	1.038	0.932
NGC 2682 0037	Mar 24	0.891	0.820	0.830	0.858	0.838	0.823	0.827	0.793	0.835	0.836	1.025	0.938
NGC 2682 0166	Mar 22	0.867	0.810	0.817	0.846	0.832	0.823	0.813	0.792	0.834	0.832	1.025	0.928
NGC 2682 0166	Mar 24	0.867	0.810	0.816	0.830	0.830	0.821	0.825	0.789	0.829	0.831	1.014	0.920
NGC 2682 4018	Mar 22	0.827	0.799	0.753	0.829	0.828	0.815	0.812	0.790	0.830	0.829	1.017	0.895
NGC 6705 0686	Mar 25	1.05	0.822	1.111	0.849	0.884	0.846	0.824	0.813	0.857	0.863	0.934	0.972
NGC 6705 0916	Mar 25	1.00	0.796	1.169	0.838	0.880	0.849	0.828	0.818	0.861	0.859	0.906	0.954
NGC 6705 1145	Mar 29	0.98	0.850	1.107	0.850	0.886	0.839	0.818	0.812	0.846	0.845	0.953	0.913
NGC 6705 1223	Mar 29	0.75	0.711	0.889	0.694	0.862	0.824	0.813	0.811	0.833	0.829	0.882	0.882
NGC 6819 0281	Mar 30	0.98	0.900	0.893	0.848	0.884	0.817	0.802	0.792	0.857	0.868	0.987	0.993
NGC 6819 0287	Mar 29	0.87	0.833	0.981	0.877	0.844	0.829	0.796	0.812	0.842	0.853	1.013	0.902
NGC 6819 0339	Mar 30	0.86	0.803	0.836	0.852	0.849	0.832	0.823	0.827	0.817	0.844	1.022	0.868
NGC 6819 1306	Mar 31	0.93	0.809	0.909	0.870	0.842	0.817	0.806	0.806	0.817	0.811	0.963	0.889

Table 3—Continued

Star Name ^a	Date Observed	(B-V) ₀ ^b	Ca4226	CN4216	Fe4065	Fe4530	Fe4680	Fe4920	Fe5011	Fe5270	Fe5335	Gband	Mg
------------------------	---------------	---------------------------------	--------	--------	--------	--------	--------	--------	--------	--------	--------	-------	----

^aIdentifications as given in the WEBDA database

^bSources for photometry and reddening:

NGC 1245: (B-V) and E(B-V)=0.25 from Burke et al. (2004)

NGC 2099: (B-V) from Kiss et al. (2001) (via WEBDA), E(B-V)=0.29 (Mermilliod et al. 1996)

NGC 2324: (B-V) from Kyeong et al. (2001) (via WEBDA), E(B-V)=0.25 (Piatti et al. 2004)

NGC 2539: (B-V) and E(B-V)=0.06 from Lapasset et al. (2000)

NGC 2682: (B-V) and E(B-V)=0.05 from Montgomery et al. (1993)

NGC 6705: (B-V) from Stetson (2000) (via WEBDA), E(B-V)=0.43 (Sung et al. 1999)

NGC 6819: (B-V) and E(B-V)=0.16 from (Rosvick & Vandenberg 1998) ((B-V) via WEBDA)

Table 4. Comparison of Indices

Subset of Data	Average of Difference for All Indices	Standard Deviation of Difference for All Indices
1.3 m & 2.4 m	0.00033	0.0335
1.3 m & 1.3 m	0.0028	0.0384
All stars	0.0011	0.0287

Table 5. Coefficients of the Fit

Index	Coefficient
Const	-3.180415
Fe4065	4.398434
CN 4216	1.105911
Ca4226	-2.480848
G-band	-0.725162
Fe4530	0
Fe4680	2.835423
Fe4920	-1.620898
Fe5011	0
Mg	0
Fe5270	0
Fe5335	0

Table 6. Derived Cluster Metallicities

Cluster Name	Star Name	(B-V) ₀	Clump Star [m/H]	Cluster [m/H]	Cluster σ
NGC 1245				-0.14	0.09
	0010	1.128	-0.043		
	0014	1.164	-0.120		
	0132	1.149	-0.163		
	0148	1.168	-0.163		
	0162	1.147	-0.287		
	0395	1.146	-0.057		
NGC 2099				+0.05	0.14
	0004	0.87	+0.297		
	0031	0.89	+0.040		
	0049	0.89	-0.198		
	0064	0.95	+0.080		
	0148	0.97	+0.059		
	0439	0.89	+0.034		
	0454	0.93	+0.102		
	0716	0.86	+0.002		
NGC 2324				-0.06	0.07
	0850	0.87	-0.065		
	0850	0.87	-0.115		
	1006	0.89	-0.102		
	1552	0.91	+0.040		
NGC 2539				-0.04	0.05
	0114	0.886	-0.078		
	0229	0.906	+0.003		
	0246	0.879	+0.009		
	0251	0.883	-0.084		
NGC 2682				-0.05	0.04
	0020	0.791	-0.061		
	0037	0.881	-0.019		
	0166	0.857	-0.001		

Table 6—Continued

Cluster Name	Star Name	(B-V) ₀	Clump Star [m/H]	Cluster [m/H]	Cluster σ
	0166	0.857	-0.091		
	4018	0.817	-0.074		
NGC 6705				+0.14	0.16
	0686	1.05	+0.144		
	0916	1.00	+0.324		
	1145	0.98	+0.157		
	1223	0.75	-0.065		
NGC 6819				+0.07	0.24
	0281	0.90	-0.273		
	0287	0.79	+0.308		
	0339	0.78	+0.082		
	1306	0.85	+0.152		